Neurobiology of Disease

Increased Citrullination of Histone H3 in Multiple Sclerosis Brain and Animal Models of Demyelination: A Role for Tumor Necrosis Factor-Induced Peptidylarginine Deiminase 4 Translocation

Fabrizio G. Mastronardi,[1] D. Denise Wood,[1] Jiang Mei,[3] Reinout Raijmakers,[4] Vivian Tseveleki,[5] Hans-Michael Dosch,[2] Lesley Probert,[5] Patrizia Casaccia-Bonnefil,[3] and Mario A. Moscarello[1]

[1]Department of Structural Biology and Biochemistry and [2]Infection, Immunity, Injury, and Repair, The Hospital for Sick Children, Toronto, Ontario, Canada M5G 1X8, [3]Department of Neuroscience and Cell Biology, Robert Wood Johnson Medical School, Piscataway, New Jersey 08854, [4]Department of Biochemistry, Nijmegen Center for Molecular Life Sciences, Radboud University Nijmegen, NL-6500 HB Nijmegen, The Netherlands, and [5]Laboratory of Molecular Genetics, Hellenic Pasteur Institute, Athens GR-115 21, Greece

Modification of arginine residues by citrullination is catalyzed by peptidylarginine deiminases (PADs), of which five are known, generating irreversible protein structural modifications. We have shown previously that enhanced citrullination of myelin basic protein contributed to destabilization of the myelin membrane in the CNS of multiple sclerosis (MS) patients. We now report increased citrullination of nucleosomal histones by PAD4 in normal-appearing white matter (NAWM) of MS patients and in animal models of demyelination. Histone citrullination was attributable to increased levels and activity of nuclear PAD4. PAD4 translocation into the nucleus was attributable to elevated tumor necrosis factor-α (TNF-α) protein. The elevated TNF-α in MS NAWM was not associated with $CD3^+$ or $CD8^+$ lymphocytes, nor was it associated with $CD68^+$ microglia/macrophages. GFAP, a measure of astrocytosis, was the only cytological marker that was consistently elevated in the MS NAWM, suggesting that TNF-α may have been derived from astrocytes. In cell cultures of mouse and human oligodendroglial cell lines, PAD4 was predominantly cytosolic but TNF-α treatment induced its nuclear translocation. To address the involvement of TNF-α in targeting PAD4 to the nucleus, we found that transgenic mice overexpressing TNF-α also had increased levels of citrullinated histones and elevated nuclear PAD4 before demyelination. In conclusion, high citrullination of histones consequent to PAD4 nuclear translocation is part of the process that leads to irreversible changes in oligodendrocytes and may contribute to apoptosis of oligodendrocytes in MS.

Key words: **multiple sclerosis; citrulline; peptidylarginine deiminase; myelin; TNF-α; histone**

Introduction

Multiple sclerosis (MS) is an inflammatory demyelinating disease of the CNS. Most studies of disease progression in the white matter of MS patients have focused on the autoimmune destructive mechanisms in CNS lesions. The identity and mechanisms of processes generating disease progression and new lesions with failures of remission and regeneration remain unknown (Mastronardi and Moscarello, 2005). We previously proposed that myelin damage in MS white matter results from a failure to maintain compact adult myelin reflecting abnormally enhanced citrullination of myelin basic protein (MBP), because these less cationic MBP isomers are unable to stabilize myelin multilayers (Moscarello et al., 1994) and are more susceptible to digestion by proteases (Pritzker et al., 2000).

Protein deimination (arginine to citrulline conversion) is mediated by a family of enzymes, the peptidylarginine deiminases (PADs) (EC 3.5.3.15), that display both tissue and substrate specificity. The PAD genes are clustered on chromosome 1 in humans (1p36.1) and syntenic regions of rodent genomes (Vossenaar et al., 2003). The main PAD enzyme expressed in the CNS is PAD2. It is found in white matter (Lamensa and Moscarello, 1993) and oligodendrocytes (Akiyama et al., 1999) in which it deiminates MBP (Wood and Moscarello, 1989; Lamensa and Moscarello, 1993) at abnormally high levels (Moscarello et al., 1994; Wood et

Received June 2, 2006; revised Sept. 21, 2006; accepted Sept. 22, 2006.

This work was supported by a research grant from the Multiple Sclerosis Society of Canada (M.A.M., F.G.M.). P.C.-B. was supported by the Multiple Sclerosis Research Foundation, National Multiple Sclerosis Society Grants RG 3421-A-4 and PP1053, and National Institutes of Health–National Institute of Neurological Disorders and Stroke Grant RO1-NS42925. R.R. was supported by Dutch Technology Foundation Grant 790.35.898. H.-M.D. was supported by Canadian Institutes of Health Research. L.P. was supported by 6th Framework Program of the European Union and Neuropromise Grant LSHM-CT-2005-018637. We thank Dr. A. Nicholas (University of Alabama at Birmingham, Birmingham, AL) for the F95 antibody. We thank Teresa Miani for technical support and Michael Ho from the Hematopoietic Stem Cell Immunopathology service laboratory for immunohistochemistry. We are grateful to Drs. R. M. Nagra and W. W. Tourtellotte and their team for providing normal and multiple sclerosis samples from the Human Brain and Spinal Fluid Resource Center's VA West Los Angeles Healthcare Center (Los Angeles, CA), which is sponsored by National Institute of Neurological Disorders and Stroke–National Institute of Mental Health, National Multiple Sclerosis Society, and the Department of Veterans Affairs.

Correspondence should be addressed to Fabrizio G. Mastronardi, Department of Structural Biology and Biochemistry, The Hospital for Sick Children, Toronto, Ontario, Canada M5G 1X8. E-mail: fabrizio@sickkids.ca.

DOI:10.1523/JNEUROSCI.3349-06.2006

 0270-6474/06/2611387-10$15.00/0

al., 1996; Kim et al., 2003). PAD4, unlike other PADs, can translocate into the nucleus (Vossenaar et al., 2003), in which it deiminates histones (Hagiwara et al., 2002; Nakashima et al., 2002; Cuthbert et al., 2004; Sarmento et al., 2004; Wang et al., 2004). The association of PAD4 activity with a number of inflammatory diseases (Nissinen et al., 2003; Lundberg et al., 2005; Makrygiannakis et al., 2006) may be an indicator of the involvement of this enzyme in cellular stress mechanisms.

Here we show that PAD4 is overexpressed and activated in the CNS of MS patients and animal models of demyelinating diseases. PAD4 translocation into the nucleus stimulated by tumor necrosis factor (TNF)-α deiminated histone (H3) in normal-appearing white matter (NAWM) of MS patients suggests a cascade that may lead to increased oligodendrocyte apoptosis. The present report on PAD4 proposes that multiple members of the PAD family may be upregulated in MS tissue, each of which contributes to the pathogenesis of MS in a particular manner.

Materials and Methods

Brain samples and fractionation. NAWM samples from brains of MS patients and white matter from controls were obtained from the MS tissue bank at the University of California, Los Angeles (F.G.M. and P.C.-B.). The samples did not contain plaque material, and each one of them was accompanied by photographic documentation of the dissected area. The clinical diagnosis, pathology, and autolysis times for the frozen white matter samples are summarized in supplemental Table 1 (available at www.jneurosci.org as supplemental material). Fractionation of brain samples into myelin (A and B), microsomal (C), and nuclear (D) fractions from white matter was performed with a modification of a previous method (Cruz and Moscarello, 1985) by differential centrifugation as described previously (Mastronardi et al., 2000).

Transgenic mice. ND4 transgenic mice have been described previously (Mastronardi et al., 1993, 1996; Moscarello et al., 2002). They contain 70 copies of the cDNA for the myelin-associated proteolipid protein (PLP) DM20. Both the TGK21 and TG6074 TNF-α transgenic mouse lines are models for primary progressive demyelination as described previously (Akassoglou et al., 1997, 1998, 1999). Mice used in this study had been backcrossed into the C57BL/6 genetic background for at least seven generations. Brain nuclear and membrane-containing fractions were prepared from normal and transgenic littermate mice as described previously for normal mice (Mastronardi et al., 2000). Animal use protocols and studies were approved by the Animal Care Committee of The Hospital for Sick Children.

Antibodies. Primary antibodies (Abs) used in this study included anti-TNF-α (Ab 1793), anti-histone H3 (Ab 1791), anti-citrullinated histone H3 (anti-H3^{cit}) (Ab 5103), all purchased from Abcam (Cambridge, MA). Antibodies against GFAP, CD3, CD8, and CD68 were purchased from DakoCytomation (Glostrup, Denmark). The polyclonal antibody to PAD isozymes (1–4) was a gift from Dr. H. Takahara (Ibaraki University, Ibaraki, Japan). This antibody cross reacts with PAD1–PAD4 (Takahara et al., 1989; Terakawa et al., 1991; Nishijyo et al., 1997; Rus'd et al., 1999). The affinity-purified isotype-specific anti-PAD4 polyclonal antibody was described previously (Vossenaar et al., 2004). Anti-citrulline IgM mouse monoclonal antibody F95 (mAb F95) was a gift from Dr. A. Nicholas (University of Alabama at Birmingham, Birmingham, AL). Anti-citrulline (modified) detection kit was purchased from Upstate Biotechnology (Lake Placid, NY). Secondary anti-mouse and anti-rabbit IgG heavy and light chain antibodies, conjugated with horseradish peroxidase (Bio-Rad, Hercules, CA), were used in Western and slot blot assays.

Immunohistochemistry. Immunohistochemistry of Formalin-fixed paraffin-embedded non-neurological control white matter and MS NAWM using anti-citrulline antibody (mAb F95) (Nicholas and Whitaker, 2002; Nicholas et al., 2005) was done according to the methods described previously (Liu et al., 2005; Nicholas et al., 2005). Immunohistochemistry using anti-GFAP, CD3, CD8, and CD68 antibodies for detection of astrocytes, lymphocytes, and activated microglia/macrophages was done with an automated Ventana Medical Systems (Tucson, AZ) Benchmark XT immunostaining system as performed by The Hospital for Sick Children Immunopathology Service laboratory using their standard operating protocols for these reagents. Luxol fast blue (LFB) histology was performed by The Hospital for Sick Children Pathology Service laboratory.

Western blots and immunoslot blot quantitation. The identity of histone H3 and histone H3 citrullinated proteins was done by Western blot analysis (Towbin et al., 1979). One polyclonal antibody recognized histone H3, and the other recognized histone H3 in which arginines 2, 8, and 17 were deiminated. The detection of PAD4 was obtained by Western blot analysis using an antibody generated against PAD4 (Vossenaar et al., 2004) (1:100 dilution). TNF-α antibody (Ab 1793) was used at a dilution of 1:1000. Ab 1793 was made against full-length native purified human TNF-α. For slot blot analysis, these antibodies were diluted 1:2000 (mouse monoclonal anti-CD68), 1:4000 (rabbit polyclonals anti-CD3 and anti-CD8), and 1:10,000 (rabbit polyclonal anti-GFAP) and incubated with human white matter homogenate, 5 μg of protein per slot. All primary and secondary antibodies were diluted in 5% nonfat dry skim milk in Tris-HCl, pH 7.5 (blotto), containing 0.05% Tween 20. Immunoreactive bands were identified with horseradish peroxidase-conjugated secondary antibodies followed by Enhanced chemiluminescence (ECL) detection (Amersham Biosciences, Piscataway, NJ) after exposure of Kodak Biomax XAR film (Eastman Kodak, New Haven, CT). For Western blots, nuclear protein extracts from MS and normal mice were prepared from nuclei isolated from frozen NAWM and whole-cell extracts of cultured cells. Proteins were separated through 10–20% tricine polyacrylamide gels (Invitrogen, Carlsbad, CA) by electrophoresis and Western blotted onto nitrocellulose membranes. The membranes were incubated with primary and secondary antibodies. The horseradish peroxidase-linked secondary antibodies were detected using ECL substrate and exposure of XAR Biomax Kodak film (Eastman Kodak).

To obtain the ratio of H3^{cit}/H3, nuclear fractions containing 5 μg of protein diluted to 100 ng/ml protein were loaded in triplicate onto wetted nitrocellulose membranes in a Biodot (slot format) ultrafiltration unit (Bio-Rad) under vacuum. The ratio of H3^{cit}/H3 was calculated from immunoslot blots after detection of H3^{cit} and H3. The nuclear fractions (D) diluted in PBS, pH 7.4, and 3 M urea were loaded onto slots in triplicate.

Determination of the ratio of H3^{cit}/H3 in mouse brain nuclear fractions was done in a similar manner to that of the human (above). Quantitation of PAD4 in nuclear protein extracts was by an immunoslot blot method. The antigens were measured in 10 μg aliquots of total protein applied to each slot. The assays for each individual were repeated three times.

Acute and chronic experimental autoimmune encephalomyelitis. SJL mice were purchased from Charles River (Montreal, Quebec, Canada), certified pathogen free, and maintained in a pathogen-free environment for 1–4 weeks before the start of experiments. Acute (aEAE) and chronic relapsing (CREAE) experimental autoimmune encephalomyelitis was induced in 6- to 8-week-old SJL female mice as described previously by us (Mastronardi et al., 2004). For induction of aEAE, 6- to 8-week-old SJL females were injected subcutaneously at the base of the tail with bovine MBP (200 μg), emulsified in complete Freund's adjuvant (CFA) (Difco, Detroit, MI). Pertussis toxin (200 ng; Sigma, St. Louis, MO) was diluted in PBS and injected intravenously via the tail vein. All mice were given a second intravenous injection of pertussis toxin 48 h later. For chronic relapsing EAE, mice were injected twice with proteolipid protein peptide 139–151 (HCLGKWLGHPDKF, 300 μg emulsified in CFA) subcutaneously. Animal use protocols and studies were approved by the Animal Care Committee of The Hospital for Sick Children.

Oli-Neu cell culture and treatments. Oli-Neu cells (a proliferating, undifferentiated, murine oligodendrocyte progenitor cell line) were differentiated in oligodendrocyte differentiation medium (ODM) containing 0.5 mg/ml cAMP for 7 d (medium was changed every 2 d). After 7 d in ODM, cells were treated with 200 ng/ml TNF-α recombinant protein for different times (0, 1, 6, 24, and 48 h). The concentration of TNF-α was based on the consideration that these concentrations best mimic a pathological condition similar to the one present *in vivo*. In addition, the use of this concentration for treatments of oligodendrocyte-derived cell cul-

tures and primary oligodendrocytes has been documented by several previous studies (Hisahara et al., 1997; Ladiwala et al., 1999; Ye and D'Ercole, 1999; Cammer, 2000; Buntinx et al., 2004b). The cells were harvested by trypsinization, and the cells that could not be trypsinized were scraped off in cold PBS containing proteinase inhibitor mixture. For quantitation of PAD4 and $H3^{cit}$/H3 ratios, cells were homogenized in PBS, pH 7.4, in 3 M urea, diluted to a final protein concentration of 0.1 mg/ml, and aliquots corresponding to 5 μg (H3 and $H3^{cit}$) and 10 μg (PAD4) of total protein by an immunoslot blot method.

Transfection of Oli-Neu cells with PAD4 cDNA. Cells were plated at a density of 1.4×10^5 cells/100 mm dish in 7 ml of medium containing 1% horse serum and then transfected with 2 μg of endotoxin-free pcDNA expressing PAD4 or with empty vector control using Fugene 6 at a ratio of 3 μl to 2 μg of DNA. Cultures were kept for 2 additional days in growth medium and then either harvested or switched to differentiation medium. Extracts were generated either 1 or 4 d later. Immunofluorescent labeling of Oli-Neu cells was done by the method described by Liu et al. (2005). The primary affinity-purified anti-PAD4 rabbit antibody was detected with an anti-rabbit red fluorophore. Nuclei were labeled with 4′,6′-diamidino-2-phenylindole (DAPI). Immunoreactive cells were analyzed using a fluorescence microscope (DM-RA; Leica, Nussloch, Germany), and the images were captured using a Hamamatsu (Shizouka, Japan) CCD camera interfaced with a G4 computer.

Statistical analysis. Data were analyzed with two-tailed parametric tests, and end points were compared by Fisher's exact test. Significance was set at 5%. Results of image analysis were analyzed by Tukey–Kramer multiple comparison tests. MS and the normal groups were compared using nonparametric two-tailed *p* value unpaired *t* tests with the Mann–Whitney test using Prism and Instat software (GraphPad Software, San Diego, CA) for the Power Mac.

Results

In this study, we analyzed NAWM tissue from MS brains and white matter from control patients to define biochemical changes that would render these regions more susceptible to subsequent lesion development. NAWM has been demonstrated to be abnormal because of several biological and histological changes and is a site of active pathology. It may represent early stages preceding demyelination. A discussion of these changes has been published by Ludwin (2006).

PAD4 is elevated in MS normal-appearing white matter

Citrullination is an irreversible, posttranslational modification of arginine residues in proteins. We have shown previously that this modification occurs on MBP from white matter of both normal and MS tissues (Moscarello et al., 1994; Kim et al., 2003), and it becomes pronounced as the disease progresses, with acute fulminating Marburg's disease the most extreme example (Wood et al., 1996).

Because immunohistochemical PAD staining revealed an elevated nuclear localization of PAD in the MS compared with control sections (data not shown), we decided to further analyze PAD subcellular localization after fractionation of NAWM samples from MS patients and control brains. White matter samples from normal and MS were thereby fractionated using previously published methods (Mastronardi et al., 2000) into the following: a membrane-containing fraction (arbitrarily denominated A + B), which contains myelin, a non-myelin microsomal fraction (called C), and a nuclear fraction (called D). Quantitation of the relative amount of binding of the anti-PAD (1–4) antibody in the normal and MS fractions (Fig. 1*A*) revealed high levels in the MS myelin fractions (A + B). The C fraction contained the smallest amount, but it was still 2.8-fold higher in patients than in the normal C fraction. Interestingly, the nuclear fraction (D) contained a 3.5-fold higher level of PAD1–PAD4 in the MS samples

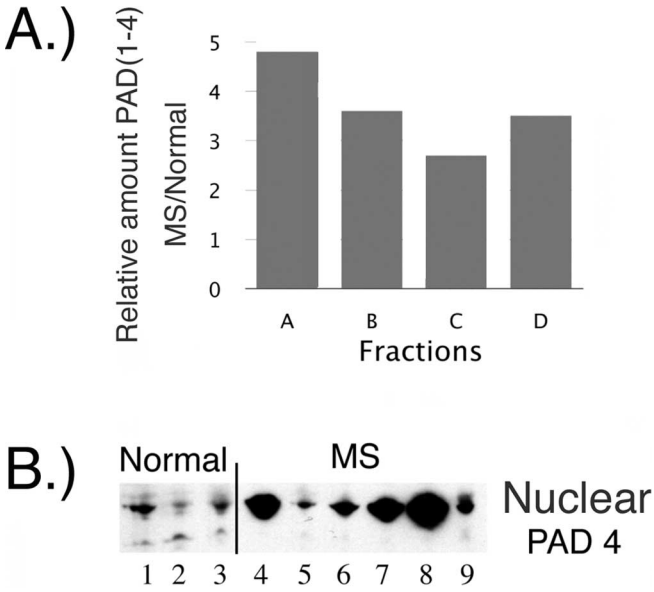

Figure 1. PAD4 in normal white matter and MS normal-appearing white matter. ***A***, The differential distribution of PAD (1–4) proteins in MS samples was confirmed by fractionation of brain extracts into membrane (A + B), microsomal (C), and nuclear (D) fractions. The amount of total PAD protein was measured, and the results are presented as a bar graph of values in MS samples relative to normal controls. ***B***, Anti-PAD4 Western blot of nuclear fraction from cortical white matter further supported the increased levels of PAD4 in the nuclear fraction of MS sample compared with the levels in normal controls. The nuclear fractions used in the PAD4 Western blot were as follows: Normal 1, 2, and 3 are HSB 3236, 3276, and 3322; MS 4–9 are HSB 3502, 2429, 3522, 3509, 2800, and 2485, respectively. These individuals are described further in supplemental Table 1 (available at www.jneurosci.org as supplemental material).

compared with normal controls, and this was most likely attributable to the nuclear PAD4 protein. Because PAD1 is found mainly in the epidermis and uterus and PAD3 in hair follicles, these observations implicated elevation of two PAD activities: PAD2, known to preferentially deiminate (or citrullinate) MBP (Lamensa and Moscarello, 1993), and nuclear PAD4, known to preferentially deiminate nucleosomal histones (Cuthbert et al., 2004; Wang et al., 2004).

To determine whether PAD4 was elevated in nuclear fractions from normal white matter and MS NAWM, we probed Western blots with anti-PAD4 antibody, which showed elevated but variable PAD4 levels in MS samples (Fig. 1*B*). These results are indicative that a nuclear PAD4 was expressed and elevated in MS NAWM.

Citrullinated histone H3 in NAWM from MS

To determine whether elevated nuclear PAD4 was accompanied by citrullination of nuclear proteins, we used a citrulline-specific monoclonal antibody (F95) to stain normal (Fig. 2*A*) and MS (Fig. 2*B*,*C*) white matter sections. The F95 staining revealed strong nuclear labeling in the MS white matter, which was less and more diffuse in the normal white matter. The increased nuclear labeling, as shown in the higher magnification (1000× oil) (Fig. 2*C*, arrows) with the anti-citrulline monoclonal antibody in the MS nuclei, was likely the result of elevated nuclear PAD4.

To substantiate that histone H3 was citrullinated, we measured citrullinated histone H3 directly with anti-histone H3 antibody (anti-$H3^{cit}$) prepared with a synthetic peptide recognizing the citrullinated sites shown in Figure 2*D*. We prepared nuclear protein fractions from various frozen normal white matter and NAWM of MS individuals to determine whether $H3^{cit}$ was ele-

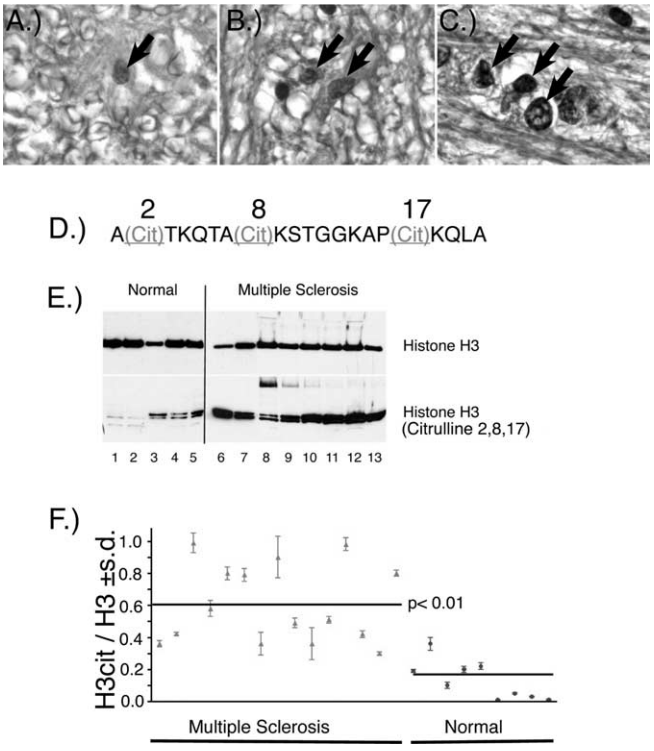

Figure 2. Citrullinated histones in normal and MS brain and nuclear fractions. Immunohistochemical staining of normal (***A***, 400×), and MS (***B***, 400×; ***C***, 1000× oil) white matter with anti-citrulline (F95) monoclonal antibody. Arrows indicate nuclear labeling with the F95 antibody. A more intense nuclear labeling was observed in the MS white matter. ***D***, The sequence of the tri-citrullinated N-terminal histone H3 peptide in which the arginyl residues at positions 2, 8, and 17 are replaced by citrulline. ***E***, Western immunoblot of nuclear fractions prepared from white matter from normal and MS individuals with anti-histone H3 and anti-H3^{cit}. ***F***, The ratio ± SD of H3^{cit}/H3 in nuclear white matter fractions from normal and individuals with MS. The mean of the H3^{cit}/H3 ratios for the MS and normal groups is indicated by the horizontal lines ($p < 0.01$, nonparametric test). A list of the clinical diagnosis for each of the samples used in these experiments and the values ± SD of the H3^{cit}/H3 ratios are provided in supplemental Table 1 (available at www.jneurosci.org as supplemental material).

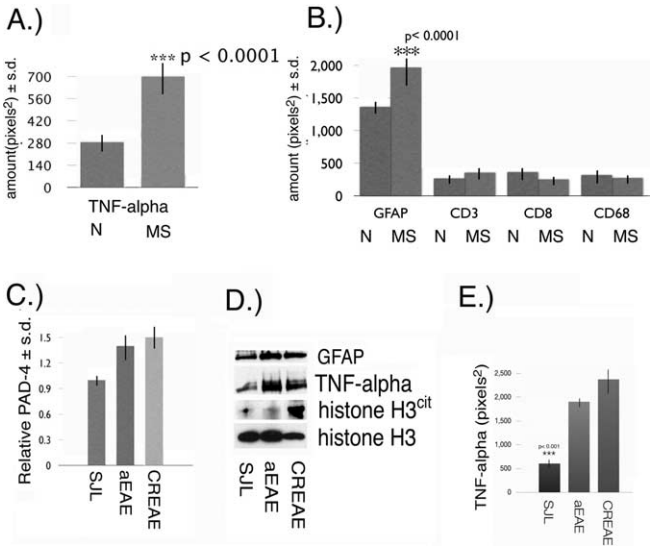

Figure 3. TNF-α and cytological markers in MS NAWM. ***A***, Quantitation of TNF-α ± SD in white matter from normal (N) ($n = 8$) and NAWM from MS patients ($n = 17$) by immunoslot blot. ***B***, Quantitation ± SD of GFAP, CD3, CD8, and CD68 levels in normal (N) white matter and MS NAWM. ***C***, Relative amount of PAD4 ± SD in brain nuclear fractions from SJL, aEAE, and CREAE mice. ***D***, Western blot of whole-brain proteins from SJL, aEAE, and CREAE mice with anti-GFAP, anti-TNF-α, anti-histone H3^{cit}, and anti-histone H3. ***E***, Amount of TNF-α ± SD ($p < 0.001$) in 5 μg of total brain proteins from SJL, aEAE, and CREAE mice.

vated in the MS cases. Abundant H3^{cit} was present in MS NAWM nuclear fractions as detected by Western blot, with only traces in white matter from controls (Fig. 2*E*). Based on these results, we calculated the ratio of H3^{cit}/H3 in the nuclear fractions prepared from a number of individuals with MS and normal controls by immunoslot blot. The scatter plot shown in Figure 2*F* revealed a variable but elevated clustering of H3^{cit}/H3 ratios for the MS group. These ratios ranged from very high proportions of H3^{cit} to moderate ratios, ~0.3. The normal individuals had H3^{cit}/H3 ratios significantly below the MS ratios. The mean of the H3^{cit}/H3 ratio for all of the MS individuals, as a group, was 0.6. That of the normal group was 0.2. The nonparametric comparison of the means of the MS group and the normal showed a significant difference, with a p value <0.01. These results suggest that the increased nuclear PAD4 in MS NAWM was associated with increased levels of citrullinated histone H3.

TNF-α in NAWM from MS patients

To determine whether the proinflammatory cytokine TNF-α, the overexpression of which induced demyelinating disease in mice (Akassoglou et al., 1999), was also elevated in MS, we quantified the amount of TNF-α in white matter from normal individuals and NAWM from MS patients ($n = 17$ MS; $n = 8$ normal). Quantitation of the amount of TNF-α for the MS group revealed a 2.4-fold increase ($p < 0.0001$) of TNF-α in NAWM (Fig. 3*A*). A possible source for TNF-α in the MS NAWM might be from inflammatory cells, such as infiltrating macrophages and/or resident microglia and activated astrocytes or a combination of all of these cell types. To determine whether any of these cells were involved, we used various cytological markers of inflammatory infiltrates to determine whether an underlying inflammation was present in MS NAWM samples. The following specific cytological markers were used: anti- GFAP to measure astrocytosis, anti-CD68 to measure microglia and/or macrophage (Ulvestad et al., 1994), and anti-CD3 (Selmaj et al., 1991) and CD8 (McDole et al., 2006) to measure lymphocyte infiltration. The results for these markers are shown in Figure 3*B* and revealed similar levels of CD3, CD8, and CD68 between MS and normal individuals. Only GFAP levels were significantly elevated (1.5-fold) in MS samples compared with controls ($p < 0.0001$). These biochemical results were further substantiated by immunohistochemical analysis (supplemental Figs. 2, 3, available at www.jneurosci.org as supplemental material). Briefly, LFB staining was done to ensure that the quality of the Formalin-fixed MS and normal white matter tissue sections were comparable and that the MS NAWM lacked detectable lesions (supplemental Fig. 1, available at www.jneurosci.org as supplemental material). Immunohistochemical analysis of white matter tissue sections revealed a variable but consistent astrocytosis (as determined by GFAP staining) in the MS NAWM sections compared with normal controls (supplemental Fig. 2, Table 2, available at www.jneurosci.org as supplemental material). CD68, to assess microglial infiltration, was barely detectable (supplemental Fig. 2, available at www.jneurosci.org as supplemental material). CD3 and CD8 stainings, to assess lymphocytic infiltration also revealed no differences between the normal and MS white matter (supplemental Fig. 3, available at www.jneurosci.org as supplemental material). Together, these results suggest that the main contribution of TNF-α in these MS cortical NAWM samples may be from astrocytes.

TNF-α and PAD4 in EAE

EAE is a T-cell-mediated disease that displays many of the immune-mediated changes found in MS. Because these molecules (CD3, CD8, and CD68) are elevated in EAE as a result of the cellular infiltration, they may contribute additional TNF-α. To determine whether there were changes in PAD4 protein levels in nuclear fractions prepared from aEAE and CREAE after disease induction, we used the anti-PAD4 antibody in immunoslot blot assays. Pooled data from untreated SJL mice and animals with aEAE induced with MBP and CREAE induced with PLP (peptide 139–151) both had a 1.5-fold increase of PAD4 compared with the control group (Fig. 3*C*). To determine whether the PAD4 increase was associated with TNF-α, we used the anti-TNF-α antibody in a Western blot of whole-brain extracts prepared from SJL, aEAE, and CREAE mice. The results showed that TNF-α was elevated in both the aEAE and CREAE models (Fig. 3*D*). Western blot of GFAP revealed an increase of GFAP in both aEAE and CREAE (Fig. 3*D*). The increase in GFAP was consistent with astrocytosis, also a feature of EAE (Mastronardi et al., 2004). Western blot analysis of H3 and $H3^{cit}$ revealed a significant increase in the proportion of $H3^{cit}$ in the CREAE brain, whereas the total histone H3 ($H3^{cit}$ + H3) was similar in SJL, aEAE, and CREAE (Fig. 3*D*). The proportion of $H3^{cit}$ in H3 was only slightly increased in the aEAE brain.

To determine whether TNF-α was elevated in the EAE brains, we measured TNF-α by immunoslot blot of whole-brain homogenates and used H3 levels to account for protein loading. The results revealed a very significant ($p < 0.001$) elevation of TNF-α in the CREAE brain by fivefold over SJL. The level of TNF-α in CREAE was also significantly above that of the aEAE ($p < 0.05$) by 1.25-fold (Fig. 3*E*). These results suggest that TNF-α may have been contributed by multiple cellular infiltrates. The EAE results revealed an association between high TNF-α and elevated nuclear PAD4 and $H3^{cit}$.

Nuclear PAD4 and TNF-α are increased before clinical disease in a primary progressive demyelinating mouse model

To address early events before the onset of demyelination in NAWM, we used the ND4 transgenic mouse model. These mice have been described previously (Mastronardi et al., 1993, 1996; Moscarello et al., 2002). They have a normal period of development up to 3 months after birth and thereafter develop a chronic progressive primary CNS demyelination. Western blots of ND4 nuclear brain extracts revealed constant PAD4 expression in nuclear fractions of nontransgenic littermate mice but a dramatic rise of nuclear PAD4 with preclinical disease (3 months) (Fig. 4*A*). The readout for the activity of nuclear PAD4 was determined by quantitating the amount of histone $H3^{cit}$, which is represented as a ratio of $H3^{cit}$/H3 in normal and ND4 mouse brain nuclear extracts from mice between 2 and 8 months of age (Fig. 4*B*). At 2 months of age, the ND4 had a similar ratio to the normal. The ND4 ratio increased 2.5-fold at 3 months (preclinical → clinical). The high ratio was sustained throughout the course of the disease, demonstrating that the increased nuclear PAD4 was observed before the onset and persisted during demyelinating disease.

TNF-α expression in total brain extracts of ND4 mice at 2, 3, 6, and 8 months of age was determined by Western blot (Fig. 4*C*). Scanning the Western blot and calculating the ratio of TNF-α/histone H3 revealed that the levels in the ND4 were elevated at all ages compared with the nontransgenic littermates. The ratios for TNF-α/H3 in the normal mouse from 2 months → 8 months increased from 0.06 to 0.6. In the ND4 mouse, TNF-α/H3 ratio at 2 months was 0.6. At 8 months, the ratio increased to 2.1. These results revealed that TNF-α at 2 months was elevated 10- and 4-fold at 3 months in the ND4 mouse, before clinical signs of demyelination. The increased levels of TNF-α and the accumulation of nuclear PAD4 and $H3^{cit}$ implied an association with disease development in the ND4 transgenic mouse.

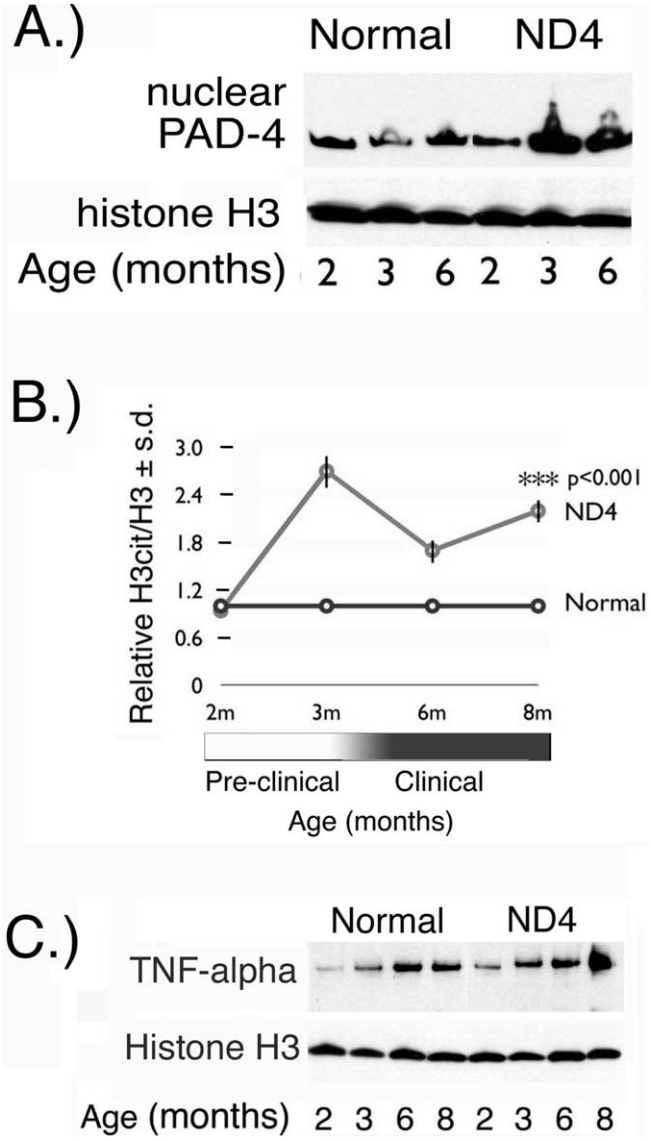

Figure 4. Nuclear PAD4 protein and TNF-α in ND4 brain. ***A***, Western blot with an anti-PAD4 polyclonal antibody of nuclear fractions prepared from 2-, 3-, and 6-month-old ND4 and normal littermates. Histone H3 immunoreactivity was used as a loading control. ***B***, Nuclear PAD4 activity was measured by determining the $H3^{cit}$/H3 ratio in ND4 brains relative to normal littermates from 2–8 months ± SD. ***C***, TNF-α Western blot of whole-brain protein homogenates from normal and ND4 littermates at 2, 3, 6, and 8 months of age. Histone H3 immunoreactivity was used as a loading control.

Mechanism of translocation of PAD4 into the nucleus

PAD4 expression was analyzed in a proliferating, undifferentiated, murine oligodendrocyte progenitor cell line, Oli-Neu (Scholze et al., 1996; Gokhan et al., 2005), to elucidate some of the factors involved in the translocation of PAD4. Immunofluorescence showed a predominantly cytoplasmic enzyme distribution and a small amount of nuclear labeling (Fig. 5*A*, red fluorophore label). After differentiation of the cells for either 1 d (Fig. 5*B*) or

5 d (Fig. 5*C*) (Gokhan et al., 2005), the localization of PAD4 was still mainly cytoplasmic, suggesting that nuclear translocation of the enzyme is not part of the constitutive differentiation program but may require exogenous signals. We considered the following.

Overexpression of PAD4

Because PAD4 levels were elevated in MS patients, we asked whether overexpression of PAD4 by itself would be sufficient for nuclear localization. Oli-Neu cells were transiently transfected with PAD4 cDNA, and nuclear enzymatic activity was measured by the formation of $H3^{cit}$ in undifferentiated and differentiated cells using the anti-$H3^{cit}$ antibody. Cellular levels of the enzyme were assessed in protein extracts from PAD4-transfected and untransfected cells by Western blot analysis (Fig. 5*D*). Immature proliferating cells contained PAD4 protein (lane 1), and transfection predictably increased PAD4 levels (lane 2). Enzymatic activity on nuclear histone was also indirectly assessed in the transfected and untransfected cells by comparing the levels of $H3^{cit}$ with actin. Because the level of $H3^{cit}$ was unchanged, overexpression of PAD4 alone was not sufficient for the translocation to the nucleus. Similar results were obtained in differentiated Oli-Neu cells (lanes 3, 4) although transfection efficiency was less. We concluded that increased cytosolic PAD4 expression is not sufficient to induce nuclear translocation but requires additional factors, e.g., TNF-α.

TNF-α signals PAD4 nuclear translocation in oligodendrocyte cell lines

Given the importance of TNF-α in demyelinating disorders (Akassoglou et al., 1997, 1998, 1999), we reasoned that TNF-α could have an important role in the translocation of PAD4 into the nucleus of oligodendrocytes, resulting in histone deimination. TNF-α treatment of Oli-Neu cells caused PAD4 to shift from a uniform cytoplasmic distribution (red label) with hardly any detectible PAD4 label in nuclei before TNF-α treatment (Fig. 5*E*). Nuclei were counterstained blue with DAPI to identify this compartment. After exposure of Oli-Neu cells with TNF-α for 30 min, a prominent redistribution of PAD4 into a vesicular compartment was found as determined by the presence of vesicular staining in the cytoplasm (Fig. 5*F*). After 60 min of TNF-α exposure, PAD4 was predominantly found in Oli-Neu nuclei (Fig. 5*G*, arrowheads). Nuclear PAD4 persisted after 24 and 48 h of continuous exposure to TNF-α (Fig. 5*H*,*I*). Besides the redistribution of PAD4 after TNF-α exposure, we also found that the levels of PAD4 protein increased. This was evident by the increased cytoplasmic staining of PAD4 in Figure 5, *H* and *I*, and by quantitation of PAD4 in Oli-Neu whole-cell extracts (Fig. 5*J*). Nuclear PAD4 activity readouts in the Oli-Neu cells was assessed by the ratio of $H3^{cit}$/H3. This was also increased by TNF-α exposure after 1 h and then increased more slowly to a maximum amount by 24–48 h (Fig. 5*K*).

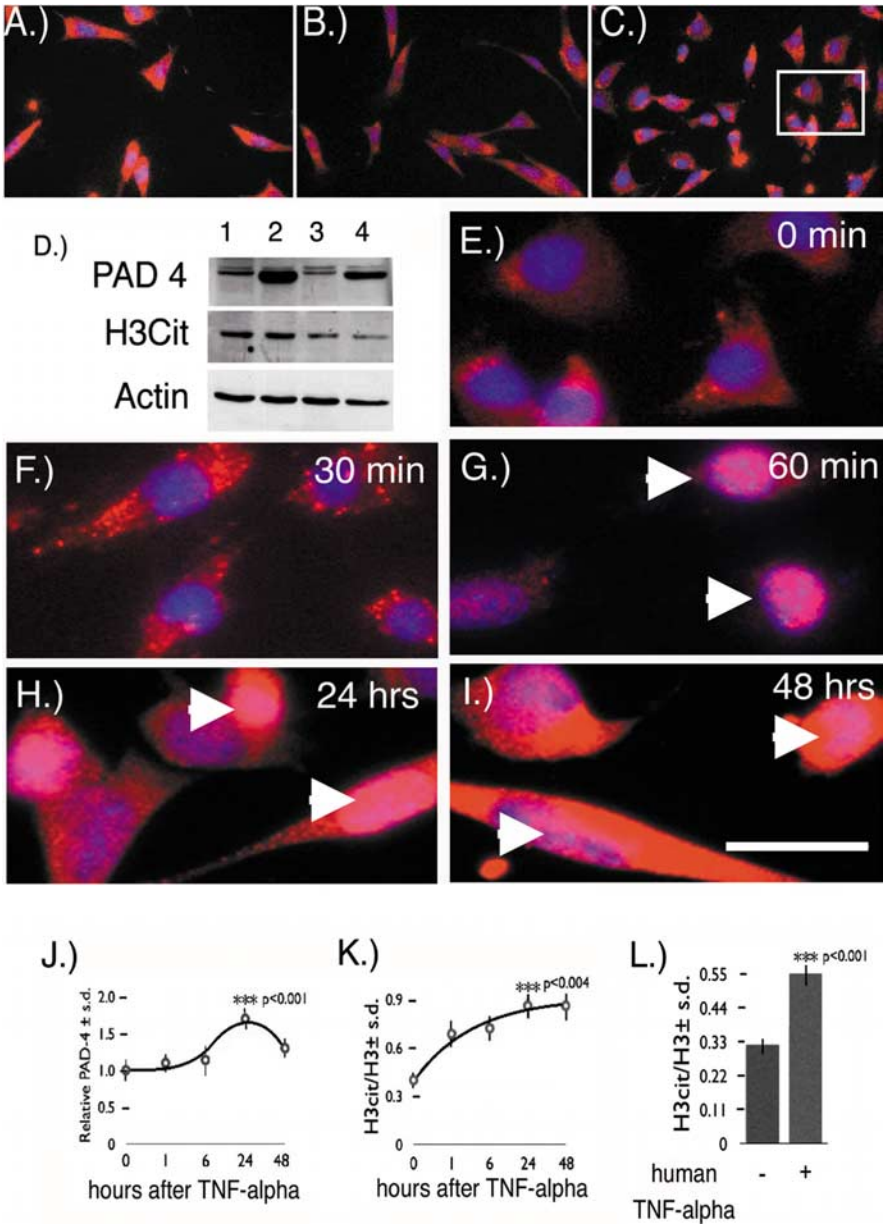

Figure 5. PAD4 subcellular localization in the Oli-Neu oligodendrocyte cell line. ***A***, PAD4 subcellular localization in immature Oli-Neu cells during growth revealed it to be cytosolic. ***B***, Oli-Neu cells 1 d in differentiation media. ***C***, Oli-Neu cells 5 d in differentiation media. The rectangle is an area magnified in ***E***. ***D***, PAD4 Western blot of cell extracts from proliferating Oli-Neu cells transfected with pcDNA plasmid (lane 1) and proliferating Oli-Neu cells transfected with mouse PAD4 cDNA in a pcDNA plasmid (lane 2). Differentiating cells transfected with pcDNA plasmid (lane 3) and differentiating cells transfected with mouse PAD4 cDNA in a pcDNA-plasmid (lane 4) are shown. $H3^{cit}$ Western blot of whole-cell extracts from proliferating Oli-Neu cells (lanes 1, 2) and differentiating Oli-Neu cells (lanes 3, 4) is shown. Actin was used as a loading control in the Western blot. ***E***, Oli-Neu cells (0 min TNF-α exposure). PAD4 was labeled with red fluorescence. Nuclei were labeled with DAPI (blue fluorescent label). ***F***, Oli-Neu cells stained for PAD4 (red label) and nuclei with DAPI (blue label) after 30 min TNF-α exposure. ***G***, PAD4 translocated into nuclei indicated by arrowheads after 60 min TNF-α exposure. ***H***, ***I***, PAD4 persisted in Oli-Neu nuclei (arrowheads) after 24 h (***H***) and 48 h (***I***). Scale bar, 50 μm. ***J***, ***K***, Quantitation of the relative amount of PAD4 (***J***) and the ratio of $H3^{cit}$/H3 in Oli-Neu cells exposed to TNF-α after 0, 1, 6, 24, and 48 h (***K***). Each time point was assayed 12 times $\pm$ SD except the 6 and 48 h times, which were assayed six times $\pm$ SD. The p values for both PAD4 levels and the $H3^{cit}$/H3 ratios were for the 0 and 24 h after TNF-α exposure. ***L***, Quantitation of the ratio of $H3^{cit}$/H3 $\pm$ SD ($p < 0.001$) in MO3-13 human oligodendrocytes exposed to recombinant human TNF-α for 24 h.

To determine whether a similar effect could be elicited on a human oligodendrocyte cell line, we exposed differentiated MO3-13 cells (McLaurin et al., 1995) with human recombinant TNF-α for 24 h and then measured histone H3^{cit}/H3 ratios. The results shown in Figure 5*L* revealed that human TNF-α was able to elicit a significant 1.67-fold ($p < 0.001$) increase in H3^{cit}/H3 ratio. The data from both differentiated Oli-Neu and MO3-13 cells are indicative that exposure to TNF-α can affect nuclear targeting of PAD4 and subsequent generation of H3^{cit}.

Nuclear PAD4 is elevated in brains from TNF-α transgenic mice

Transgenic mice that have CNS-specific overexpression of a murine TNF-α transgene (the Tg6074 line) or astrocyte-targeted expression of a tethered transmembrane human TNF-α ligand (the TgK21 line) (Akassoglou et al., 1999) were used to determine whether elevated TNF-α affected PAD4 nuclear activity directly. Both the TGK21 and TG6074 TNF-α transgenic mouse lines undergo a preclinical phase in which they are indistinguishable from nontransgenic littermates and thereafter show neurological signs of primary progressive demyelination (Akassoglou et al., 1999). The TGK21 line is preclinical at 2 weeks and displays severe symptoms of demyelination by 4 weeks. The TG6074 line is normal up to 4 weeks and shows signs of severe demyelination by 6 weeks. To confirm that these mice overexpress TNF-α protein, we measured TNF-α using the anti-TNF-α antibody (Ab 1793) in a slot blot assay of whole-brain homogenates. The results shown in Figure 6*A* revealed a significant increase of TNF-α in the preclinical and clinical phases of both TGK21 and TG6074 mice ($p < 0.001$) compared with nontransgenic littermates. Therefore, to address the question whether PAD4 was elevated in nuclear fractions before clinical signs and during disease progression, we analyzed PAD4 levels in nuclear fractions from these mice and compared them with their nontransgenic littermates. We found that the levels of nuclear PAD4 was elevated in both preclinical and clinical phases of disease correlated with increased expression of the transgene (Fig. 6*B*), with mean levels for both lines being 1.8 ± 0.4-fold higher than nontransgenic littermates. As a group, the TNF-α transgenic mice had an H3^{cit}/H3 ratio of 0.47 ± 0.01 compared with 0.24 ± 0.01 for the littermates (Fig. 6*C*). These data suggest that TNF-α has a role in the translocation of PAD4 into the nucleus from the cytoplasm.

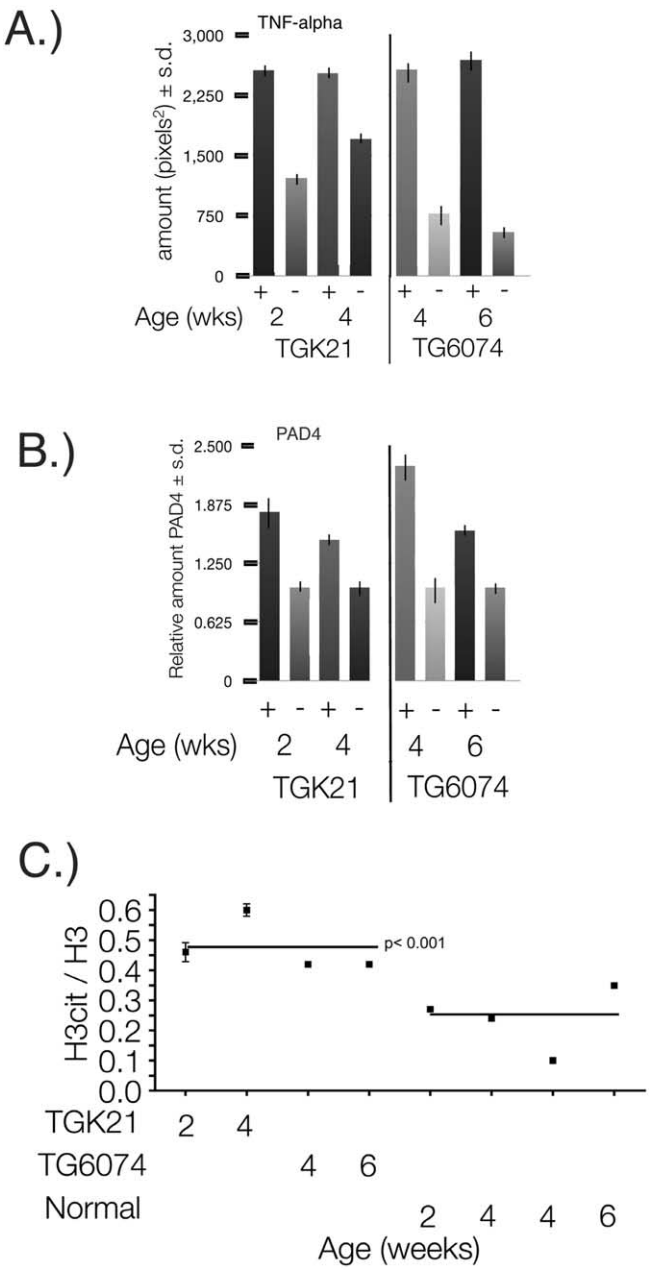

Figure 6. Nuclear PAD4 and TNF-α in TGK21and TG6074 brains. ***A***, Quantitation of TNF-α in whole-brain homogenates from TGK21 (+), TG6074 (+), and nontransgenic littermates (−) from 2-week-old TGK21 (preclinical), 4-week-old TGK21 (clinical), 4-week-old TG6074 (preclinical), and 6-week-old TG6074 (clinical) mice ($p < 0.001$). ***B***, Relative PAD4 levels in TGK21 (+) and TG6074 (+) transgenic mouse brains compared with nontransgenic (−) littermates at 2, 4, and 6 weeks of age. ***C***, Ratios of nuclear citrullinated proteins/H3 ± SD in brain nuclear protein extracts from individual TGK21 (+) and TG6074 (+) transgenic mice compared with nontransgenic littermates (−). The means of the H3^{cit}/H3 ratios for the TGK21and TG6074 transgenic mouse groups compared with their nontransgenic littermates are represented by the horizontal lines ($p < 0.001$, nonparametric test).

Discussion

Higher-order protein structures induced by posttranslational modifications are often associated with reversible events involved in signal transduction. Many modifications, however, are not reversible and invoke new primary structures not encoded by the genome. One of these modifications, deimination of proteins, the conversion of positively charged arginine to a neutral citrulline, is recently gaining more prominence as an activator and indicator of autoimmune disease (Vossenaar et al., 2003).

The failure to remyelinate involves not only early developmental molecules (John et al., 2002; Mastronardi et al., 2003, 2004; Mastronardi and Moscarello, 2005) but also an intracellular PAD (PAD4), which deiminates histones in oligodendrocytes. We demonstrate here that PAD4 levels and activity are elevated in NAWM of MS patients. We further show that PAD4 accumulates in the nuclei of cells in the white matter, in which it catalyzes the conversion of arginine to citrulline in the tail of nucleosomal histones, thereby affecting the integrity of histone–chromatin interactions. Higher-order genomic DNA structure and gene regulation is controlled by histone proteins. Histones are highly basic nuclear proteins that are subject to posttranslational modifications that can be reversible. These include acetylation, deacetylation, and methylation of N-terminal lysine residues (Roth and Allis, 1996; Svaren and Horz, 1996; Zhang and Reinberg, 2001). Deimination of arginine residues on histones are irreversible modifications that alter their net positive charge. As a result, deiminated histones have altered intermolecular interactions with proteins and likely with DNA (Sarmento et al., 2004). Because changes in the secondary structure of nucleosomal his-

tones modulate cell-specific gene expression (Ensoli et al., 1999; Brooks, 2005; Scalabrino, 2005), we propose that the increased PAD4 nuclear activity could be part of either the demyelinating process or part of a failed repair

In support of the idea that citrullinated histone affects the chromatin structure in patients, we also found that HP1-α, a protein that has an important role in chromatin compaction (Verschure et al., 2005), was decreased in NAWM from MS tissue. Although the effects of these changes on differentiation are not known, it has been shown that changes in the acetylation state of histones affect the ability of oligodendrocyte progenitors to differentiate into myelinating cells both *in vitro* and *in vivo* (Marin-Husstege et al., 2002; Shen et al., 2005). In addition, PAD4 has been suggested to be a regulator of the pS2 promoter by histone deimination, a promoter that responds to estrogen stimulation (Wang et al., 2004; Denman, 2005; Kearney et al., 2005), which in turn is suggested to be involved in many diseases, including multiple sclerosis. Deimination of arginine in histones by PAD4 has been demonstrated in other cell types (Cuthbert et al., 2004; Wang et al., 2004) to render the histones more susceptible to degradation, as demonstrated for citrullinated MBP (Pritzker et al., 2000; D'Souza et al., 2005). Together, the evidence is indicative that changes in the secondary structure of histones attributable to PAD4 translocation could either interfere with myelin biosynthesis and remyelination or could affect cell survival.

The role of TNF-α in PAD4 translocation was demonstrated *in vitro* in the Oli-Neu oligodendrocyte cell line, because incubation of the cells with TNF-α was shown to translocate PAD4 into the nucleus within 1 h. This translocation of a protein involved in regulating gene expression is reminiscent of several other proteins, including a prototypical transcription factor, nuclear factor κB (NF-κB), that dissociates from its partner Iκ-B on TNF-α activation, exposing a nuclear localization signal and allowing translocation of the protein to the nucleus (Fagerlund et al., 2005). Our results with the overexpression of PAD4 in Oli-Neu cells were indicative that overexpression was not sufficient to target PAD4 into the nucleus. This suggests that, like NF-κB, PAD4 may be sequestered cytoplasmically, released, and then targeted to the nucleus after a TNF-α inductive signal.

Because of the role of TNF-α in apoptosis of oligodendrocyte cell lines (Buntinx et al., 2004a,b) in MS brain (Raine et al., 1998), we propose here that PAD4 activity may affect oligodendrocyte survival by inducing the progressive accumulation of deiminated histones. If the histone deimination were kept unchecked, this would lead to irreversible nuclear changes and finally apoptotic death. In animal models of MS that spontaneously demyelinate, such as transgenic ND4, TGK21, and TG6074 mice, both TNF-α and PAD4 were elevated before clinical disease. More importantly, nuclear PAD4 was elevated in the transgenic mouse brains before clinical signs of demyelination, suggesting that these molecules have important roles in the pathogenesis of demyelinating diseases.

TNF-α expression in transgenic mice has been shown to be sufficient to induce non-immune-mediated demyelination (Probert et al., 1995; Kassiotis et al., 1999). Because TNF-α is expressed by astrocytes and macrophages (Chung et al., 1991) and because TNF-α also promotes proliferation of astrocytes (Selmaj et al., 1990), we propose the existence of a TNF-α feed-forward loop that would supposedly fuel the cycle of a persistent inflammatory state and induce the nuclear translocation of PAD4 in oligodendrocytes.

The pathogenesis of MS is complex. Our studies have suggested that the PAD enzymes, of which five are known, have important roles in this disease. Of the five PAD enzymes, we have shown that PAD2 is involved primarily with demyelination resulting from the deimination of MBP. Although PAD4 is a cytoplasmic enzyme, it is translocated to the nucleus in which it deiminates histones, a process that is increased in MS patients. Chromatin compaction is affected with subsequent disruption of the biosynthetic machinery of the cell. Therefore, PAD4 appears to be involved in epigenetic mechanisms in MS that may include demyelination and failed remyelination. In this report, we showed an association of increased PAD4 with increased $H3^{cit}$ and TNF-α in MS NAWM and in the brains of animal models of demyelination. The mechanism involves translocation of PAD4 $\rightarrow$ nucleus, which is mediated by TNF-α. Overexpression of PAD4 alone does not induce its translocation. Furthermore, chronic TNF-α exposure of oligodendrocyte cells in culture induced increased PAD4 protein. These studies suggest that nuclear PAD4 contributes to the pathogenesis of MS and possibly other inflammatory diseases involving TNF-α and histone deimination (A. Suzuki et al., 2003; K. Suzuki et al., 2003).

References

Akassoglou K, Probert L, Kontogeorgos G, Kollias G (1997) Astrocyte-specific but not neuron-specific transmembrane TNF triggers inflammation and degeneration in the central nervous system of transgenic mice. J Immunol 158:438–445.

Akassoglou K, Bauer J, Kassiotis G, Pasparakis M, Lassmann H, Kollias G, Probert L (1998) Oligodendrocyte apoptosis and primary demyelination induced by local TNF/p55TNF receptor signaling in the central nervous system of transgenic mice: models for multiple sclerosis with primary oligodendrogliopathy. Am J Pathol 153:801–813.

Akassoglou K, Bauer J, Kassiotis G, Lassmann H, Kollias G, Probert L (1999) Transgenic models of TNF induced demyelination. Adv Exp Med Biol 468:245–259.

Akiyama K, Sakurai Y, Asou H, Senshu T (1999) Localization of peptidylarginine deiminase type II in a stage-specific immature oligodendrocyte from rat cerebral hemisphere. Neurosci Lett 274:53–55.

Brooks WH (2005) Autoimmune disorders result from loss of epigenetic control following chromosome damage. Med Hypotheses 64:590–598.

Buntinx M, Moreels M, Vandenabeele F, Lambrichts I, Raus J, Steels P, Stinissen P, Ameloot M (2004a) Cytokine-induced cell death in human oligodendroglial cell lines. I. Synergistic effects of IFN-gamma and TNF-alpha on apoptosis. J Neurosci Res 76:834–845.

Buntinx M, Gielen E, Van Hummelen P, Raus J, Ameloot M, Steels P, Stinissen P (2004b) Cytokine-induced cell death in human oligodendroglial cell lines. II. Alterations in gene expression induced by interferon-gamma and tumor necrosis factor-alpha. J Neurosci Res 76:846–861.

Cammer W (2000) Effects of TNFalpha on immature and mature oligodendrocytes and their progenitors in vitro. Brain Res 864:213–219.

Chung IY, Norris JG, Benveniste EN (1991) Differential tumor necrosis factor alpha expression by astrocytes from experimental allergic encephalomyelitis-susceptible and -resistant rat strains. J Exp Med 173:801–811.

Cruz TF, Moscarello MA (1985) Characterization of myelin fractions from human brain white matter. J Neurochem 44:1411–1418.

Cuthbert GL, Daujat S, Snowden AW, Erdjument-Bromage H, Hagiwara T, Yamada M, Schneider R, Gregory PD, Tempst P, Bannister AJ, Kouzarides T (2004) Histone deimination antagonizes arginine methylation. Cell 118:545–553.

Denman RB (2005) PAD: the smoking gun behind arginine methylation signaling? BioEssays 27:242–246.

D'Souza CA, Wood DD, She YM, Moscarello MA (2005) Autocatalytic cleavage of myelin basic protein: an alternative to molecular mimicry. Biochemistry 44:12905–12913.

Ensoli F, Fiorelli V, Muratori DS, De Cristofaro M, Vincenzi L, Topino S, Novi A, Luzi G, Sirianni MC (1999) Immune-derived cytokines in the nervous system: epigenetic instructive signals or neuropathogenic mediators? Crit Rev Immunol 19:97–116.

Fagerlund R, Kinnunen L, Kohler M, Julkunen I, Melen K (2005) NF-κB is transported into the nucleus by importin α3 and importin α4. J Biol Chem 280:15942–15951.

Gokhan S, Marin-Husstege M, Yung SY, Fontanez D, Casaccia-Bonnefil P, Mehler MF (2005) Combinatorial profiles of oligodendrocyte-selective classes of transcriptional regulators differentially modulate myelin basic protein gene expression. J Neurosci 25:8311–8321.

Hagiwara T, Nakashima K, Hirano H, Senshu T, Yamada M (2002) Deimination of arginine residues in nucleophosmin/B23 and histones in HL-60 granulocytes. Biochem Biophys Res Commun 290:979–983.

Hisahara S, Shoji S, Okano H, Miura M (1997) ICE/CED-3 family executes oligodendrocyte apoptosis by tumor necrosis factor. J Neurochem 69:10–20.

John GR, Shankar SL, Shafit-Zagardo B, Massimi A, Lee SC, Raine CS, Brosnan CF (2002) Multiple sclerosis: re-expression of a developmental pathway that restricts oligodendrocyte maturation. Nat Med 8:1115–1121.

Kassiotis G, Bauer J, Akassoglou K, Lassmann H, Kollias G, Probert L (1999) A tumor necrosis factor-induced model of human primary demyelinating diseases develops in immunodeficient mice. Eur J Immunol 29:912–917.

Kearney PL, Bhatia M, Jones NG, Yuan L, Glascock MC, Catchings KL, Yamada M, Thompson PR (2005) Kinetic characterization of protein arginine deiminase 4: a transcriptional corepressor implicated in the onset and progression of rheumatoid arthritis. Biochemistry 44: 10570–10582.

Kim JK, Mastronardi FG, Wood DD, Lubman DM, Zand R, Moscarello MA (2003) Multiple sclerosis: an important role for post-translational modifications of myelin basic protein in pathogenesis. Mol Cell Proteomics 2:453–462.

Ladiwala U, Li H, Antel JP, Nalbantoglu J (1999) p53 induction by tumor necrosis factor-alpha and involvement of p53 in cell death of human oligodendrocytes. J Neurochem 73:605–611.

Lamensa JW, Moscarello MA (1993) Deimination of human myelin basic protein by a peptidylarginine deiminase from bovine brain. J Neurochem 61:987–996.

Liu A, Stadelmann C, Moscarello M, Bruck W, Sobel A, Mastronardi FG, Casaccia-Bonnefil P (2005) Expression of stathmin, a developmentally controlled cytoskeleton-regulating molecule, in demyelinating disorders. J Neurosci 25:737–747.

Ludwin SK (2006) The pathogenesis of multiple sclerosis: relating human pathology to experimental studies. J Neuropathol Exp Neurol 65:305–318.

Lundberg K, Nijenhuis S, Vossenaar ER, Palmblad K, van Venrooij WJ, Klareskog L, Zendman AJ, Harris HE (2005) Citrullinated proteins have increased immunogenicity and arthritogenicity and their presence in arthritic joints correlates with disease severity. Arthritis Res Ther 7:R458–R467.

Makrygiannakis D, Af Klint E, Lundberg IE, Lofberg R, Ulfgren AK, Klareskog L, Catrina AI (2006) Citrullination is an inflammation dependent process. Ann Rheum Dis 65:1219–1222.

Marin-Husstege M, Muggironi M, Liu A, Casaccia-Bonnefil P (2002) Histone deacetylase activity is necessary for oligodendrocyte lineage progression. J Neurosci 22:10333–10345.

Mastronardi FG, Moscarello MA (2005) Molecules affecting myelin stability: a novel hypothesis regarding the pathogenesis of multiple sclerosis. J Neurosci Res 80:301–308.

Mastronardi FG, Ackerley CA, Arsenault L, Roots BI, Moscarello MA (1993) Demyelination in a transgenic mouse: a model for multiple sclerosis. J Neurosci Res 36:315–324.

Mastronardi FG, Mak B, Ackerley CA, Roots BI, Moscarello MA (1996) Modifications of myelin basic protein in DM20 transgenic mice are similar to those in myelin basic protein from multiple sclerosis. J Clin Invest 97:349–358.

Mastronardi FG, Dimitroulakos J, Kamel-Reid S, Manoukian AS (2000) Co-localization of patched and activated sonic hedgehog to lysosomes in neurons. NeuroReport 11:581–585.

Mastronardi FG, daCruz LA, Wang H, Boggs J, Moscarello MA (2003) The amount of sonic hedgehog in multiple sclerosis white matter is decreased and cleavage to the signaling peptide is deficient. Mult Scler 9:362–371.

Mastronardi FG, Min W, Wang H, Winer S, Dosch M, Boggs JM, Moscarello MA (2004) Attenuation of experimental autoimmune encephalomyelitis and nonimmune demyelination by IFN-beta plus vitamin B12: treatment to modify notch-1/sonic hedgehog balance. J Immunol 172:6418–6426.

McDole J, Johnson AJ, Pirko I (2006) The role of CD8+ T-cells in lesion formation and axonal dysfunction in multiple sclerosis. Neurol Res 28:256–261.

McLaurin J, Trudel GC, Shaw IT, Antel JP, Cashman NR (1995) A human glial hybrid cell line differentially expressing genes subserving oligodendrocyte and astrocyte phenotype. J Neurobiol 26:283–293.

Moscarello MA, Wood DD, Ackerley C, Boulias C (1994) Myelin in multiple sclerosis is developmentally immature. J Clin Invest 94:146–154.

Moscarello MA, Pritzker L, Mastronardi FG, Wood DD (2002) Peptidylarginine deiminase: a candidate factor in demyelinating disease. J Neurochem 81:335–343.

Nakashima K, Hagiwara T, Yamada M (2002) Nuclear localization of peptidylarginine deiminase V and histone deimination in granulocytes. J Biol Chem 277:49562–49568.

Nicholas AP, Whitaker JN (2002) Preparation of a monoclonal antibody to citrullinated epitopes: its characterization and some applications to immunohistochemistry in human brain. Glia 37:328–336.

Nicholas AP, Sambandam T, Echols JD, Barnum SR (2005) Expression of citrullinated proteins in murine experimental autoimmune encephalomyelitis. J Comp Neurol 486:254–266.

Nishijyo T, Kawada A, Kanno T, Shiraiwa M, Takahara H (1997) Isolation and molecular cloning of epidermal- and hair follicle-specific peptidylarginine deiminase (type III) from rat. J Biochem (Tokyo) 121:868–875.

Nissinen R, Paimela L, Julkunen H, Tienari PJ, Leirisalo-Repo M, Palosuo T, Vaarala O (2003) Peptidylarginine deiminase, the arginine to citrulline converting enzyme, is frequently recognized by sera of patients with rheumatoid arthritis, systemic lupus erythematosus and primary Sjogren syndrome. Scand J Rheumatol 32:337–342.

Pritzker LB, Joshi S, Gowan JJ, Harauz G, Moscarello MA (2000) Deimination of myelin basic protein. 1. Effect of deimination of arginyl residues of myelin basic protein on its structure and susceptibility to digestion by cathepsin D. Biochemistry 39:5374–5381.

Probert L, Akassoglou K, Pasparakis M, Kontogeorgos G, Kollias G (1995) Spontaneous inflammatory demyelinating disease in transgenic mice showing central nervous system-specific expression of tumor necrosis factor alpha. Proc Natl Acad Sci USA 92:11294–11298.

Raine CS, Bonetti B, Cannella B (1998) Multiple sclerosis: expression of molecules of the tumor necrosis factor ligand and receptor families in relationship to the demyelinated plaque. Rev Neurol (Paris) 154:577–585.

Roth SY, Allis CD (1996) Histone acetylation and chromatin assembly: a single escort, multiple dances? Cell 87:5–8.

Rus'd AA, Ikejiri Y, Ono H, Yonekawa T, Shiraiwa M, Kawada A, Takahara H (1999) Molecular cloning of cDNAs of mouse peptidylarginine deiminase type I, type III and type IV, and the expression pattern of type I in mouse. Eur J Biochem 259:660–669.

Sarmento OF, Digilio LC, Wang Y, Perlin J, Herr JC, Allis CD, Coonrod SA (2004) Dynamic alterations of specific histone modifications during early murine development. J Cell Sci 117:4449–4459.

Scalabrino G (2005) Cobalamin (vitamin B(12)) in subacute combined degeneration and beyond: traditional interpretations and novel theories. Exp Neurol 192:463–479.

Scholze A, Gotz B, Faissner A (1996) Glial cell interactions with tenascin-C: adhesion and repulsion to different tenascin-C domains is cell type related. Int J Dev Neurosci 14:315–329.

Selmaj K, Raine CS, Cannella B, Brosnan CF (1991) Identification of lymphotoxin and tumor necrosis factor in multiple sclerosis lesions. J Clin Invest 87:949–954.

Selmaj KW, Farooq M, Norton WT, Raine CS, Brosnan CF (1990) Proliferation of astrocytes in vitro in response to cytokines. A primary role for tumor necrosis factor. J Immunol 144:129–135.

Shen S, Li J, Casaccia-Bonnefil P (2005) Histone modifications affect timing of oligodendrocyte progenitor differentiation in the developing rat brain. J Cell Biol 169:577–589.

Suzuki A, Yamada R, Chang X, Tokuhiro S, Sawada T, Suzuki M, Nagasaki M, Nakayama-Hamada M, Kawaida R, Ono M, Ohtsuki M, Furukawa H, Yoshino S, Yukioka M, Tohma S, Matsubara T, Wakitani S, Teshima R, Nishioka Y, Sekine A, et al. (2003) Functional haplotypes of PADI4, encoding citrullinating enzyme peptidylarginine deiminase 4, are associated with rheumatoid arthritis. Nat Genet 34:395–402.

Suzuki K, Sawada T, Murakami A, Matsui T, Tohma S, Nakazono K, Takemura M, Takasaki Y, Mimori T, Yamamoto K (2003) High diagnostic performance of ELISA detection of antibodies to citrullinated antigens in rheumatoid arthritis. Scand J Rheumatol 32:197–204.

Svaren J, Horz W (1996) Regulation of gene expression by nucleosomes. Curr Opin Genet Dev 6:164–170.

Takahara H, Tsuchida M, Kusubata M, Akutsu K, Tagami S, Sugawara K (1989) Peptidylarginine deiminase of the mouse. Distribution, properties, and immunocytochemical localization. J Biol Chem 264:13361–13368.

Terakawa H, Takahara H, Sugawara K (1991) Three types of mouse peptidylarginine deiminase: characterization and tissue distribution. J Biochem (Tokyo) 110:661–666.

Towbin H, Staehelin T, Gordon J (1979) Electrophoretic transfer of proteins from polyacrylamide gels to nitrocellulose sheets: procedure and some applications. Proc Natl Acad Sci USA 76:4350–4354.

Ulvestad E, Williams K, Mork S, Antel J, Nyland H (1994) Phenotypic differences between human monocytes/macrophages and microglial cells studied in situ and in vitro. J Neuropathol Exp Neurol 53:492–501.

Verschure PJ, van der Kraan I, de Leeuw W, van der Vlag J, Carpenter AE, Belmont AS, van Driel R (2005) In vivo HP1 targeting causes large-scale chromatin condensation and enhanced histone lysine methylation. Mol Cell Biol 25:4552–4564.

Vossenaar ER, Zendman AJ, van Venrooij WJ, Pruijn GJ (2003) PAD, a growing family of citrullinating enzymes: genes, features and involvement in disease. BioEssays 25:1106–1118.

Vossenaar ER, Radstake TR, van der Heijden A, van Mansum MA, Dieteren C, de Rooij DJ, Barrera P, Zendman AJ, van Venrooij WJ (2004) Expression and activity of citrullinating peptidylarginine deiminase enzymes in monocytes and macrophages. Ann Rheum Dis 63:373–381.

Wang Y, Wysocka J, Sayegh J, Lee YH, Perlin JR, Leonelli L, Sonbuchner LS, McDonald CH, Cook RG, Dou Y, Roeder RG, Clarke S, Stallcup MR, Allis CD, Coonrod SA (2004) Human PAD4 regulates histone arginine methylation levels via demethylimination. Science 306:279–283.

Wood DD, Moscarello MA (1989) The isolation, characterization, and lipid-aggregating properties of a citrulline containing myelin basic protein. J Biol Chem 264:5121–5127.

Wood DD, Bilbao JM, O'Connors P, Moscarello MA (1996) Acute multiple sclerosis (Marburg type) is associated with developmentally immature myelin basic protein. Ann Neurol 40:18–24.

Ye P, D'Ercole AJ (1999) Insulin-like growth factor I protects oligodendrocytes from tumor necrosis factor-alpha-induced injury. Endocrinology 140:3063–3072.

Zhang Y, Reinberg D (2001) Transcription regulation by histone methylation: interplay between different covalent modifications of the core histone tails. Genes Dev 15:2343–2360.